

Occurrence of Sharp Hydrogen Effusion Peaks of Hydrogenated Amorphous Silicon Film and Its Connection to Void Structures

Sahar Jafari,* Jonathan Steffens, Michael Wendt, Barbara Terheiden, Sylke Meyer, and Dominik Lausch

The amount of hydrogen released from plasma-enhanced chemical vapor (PECVD) deposited hydrogenated amorphous silicon (a-Si:H) layers is determined by gas effusion measurements. A sharp peak (SP) is observed in the effusion spectra of samples with substrate temperature $T_S \geq 200$ °C. Light microscopic images indicate the formation of bubbles after deposition for all samples and film deterioration after effusion measurement in correlation with the presence of the hydrogen SPs. Change in substrate temperature varies with the microstructure of the film, the hydrogen concentration, and the density. A low T_S leads to a porous structure with large number of interface bubbles, and therefore no hydrogen-induced SP appears during hydrogen effusion. Whereas high T_S causes a compact a-Si:H film in which the hydrogen effusion is limited by the longer diffusion, while the number of interface bubbles decreases. The storage of near substrate hydrogen in the bubbles in compact material leads to a local explosion by increase in excessive pressure. The difference between the low temperature peak and the position of the SP in the effusion spectra indicates the time required to fill the interface bubbles with hydrogen, which decreases with increasing film density, suggesting that the volume of the interface bubble decreases.

concentration up to 40 at%.^[1] These hydrogenated films are subjected to temperature annealing processes like rapid thermal processing (RTP) or rapid thermal annealing (RTA). The impact of firing temperature on the hydrogen diffusion and effusion is therefore of great interest. To improve the fundamental understanding of such mechanisms, knowledge of the hydrogen concentration in combination with the hydrogen diffusivity is necessary.


Frequently used characterization methods for the monitoring of hydrogen are glow-discharge optical emission spectroscopy (GD-OES), Fourier-transform infrared spectroscopy (FTIR), secondary ion mass spectroscopy (SIMS), elastic recoil detection analysis (ERDA), and nuclear reaction analysis (NRA).^[2–6] All these methods have advantages and disadvantages i.e., the latter three are usually difficult to access or costly and time consuming. A further method is an effusion analysis as reported, e.g., by

Beyer.^[7] Recently, we have reported about a simplified setup.^[8] With this setup, the kinetics of the hydrogen effusion and diffusion can be determined in combination with various heat ramp profiles as they also occur during production processes. During analyzing the effusion spectra, the phenomena of single sharp peaks (SPs) have occurred. The relationship between hydrogen peaks during effusion measurement and interface bubbles was observed, but no detailed study of these phenomena with regards to substrate temperature during the film deposition has been undertaken.^[9–11]

1. Introduction

For the past few years, there has been a rapid rise in investigation on the influence of hydrogen on the optical and electrical properties of semiconductor devices like silicon solar cells. At low temperature, plasma-enhanced chemical vapor (PECVD)-deposited passivation layers are used as a-SiN:H as an industrial standard passivation material or an intrinsic a-Si:H with large application in the solar cells. They contain hydrogen

S. Jafari, M. Wendt, Dr. S. Meyer, Dr. D. Lausch
Materials and Processes
Fraunhofer Center for Silicon Photovoltaics CSP
Otto-Eißfeldt-Straße 12, 06120 Halle, Germany
E-mail: sahar.jafari@csp.fraunhofer.de

 The ORCID identification number(s) for the author(s) of this article can be found under <https://doi.org/10.1002/pssb.202000097>.

© 2020 The Authors. Published by WILEY-VCH Verlag GmbH & Co. KGaA, Weinheim. This is an open access article under the terms of the Creative Commons Attribution License, which permits use, distribution and reproduction in any medium, provided the original work is properly cited.

DOI: 10.1002/pssb.202000097

S. Jafari
Technologies of Photovoltaics
Department of Electrical, Mechanical and Industrial Engineering (EMW)
Anhalt University of Applied Sciences HSA
Bernburger Straße 55, 06366 Köthen, Germany

J. Steffens, Dr. B. Terheiden
Department of Physics
University of Konstanz
Universitätsstr. 10, 78457 Konstanz, Germany

Dr. D. Lausch
DENKweit GmbH
Marthastraße 13, 06108 Halle, Germany

Beyer and coworkers mentioned that a type of effusion spike occurring at rather high temperatures which they attributed to crystallization during annealing.^[12,13]

Shanks and Ley observed the formation of bubbles at the interface of c-Si/a-Si from 350 °C anneal temperature and indicated that the diameter of the blister is proportional to the film thickness, and the number of bubbles is proportional to the hydrogen concentration.^[9]

There are two views that describe hydrogen diffusion through the film in terms of microstructures and cavities. In the classic view, the effusion of hydrogen is considered as a mechanism of hydrogen transport from the breaking of the Si–H bond and the shrinkage of the network, whereas in the second view, an additional transport mechanism is represented by a movement of the diffusing hydrogenated vacancies or open volumes. Beyer claimed that an interruption of the Si–Si network with hydrogen depending on H concentration, which induces the diffusion of H or H₂ through the film at high temperatures.^[7]

In contrast, Smets et al. suggested that void structure is changing depending on the density of the film during deposition from vacancies to the microscopic voids.^[14,15] Further studies have shown that annealing can cause changes in the void structure. This means that the vacancies with various forms agglomerate into nanoscale voids and diffuse out of the film at high temperatures, followed by crystallization in the film.^[16,17]

At present, the thermal stability of hydrogenated layers and the role of microstructure on hydrogen passivation of crystalline Si for the application of solar cells are of great interest, so that an investigation of the hydrogen effusion at elevated temperatures of such compounds has been conducted. Within this article, the microscopic cause of hydrogen SPs in the effusion spectra in relation to the substrate temperature T_S with the example of a-Si:H layers has been investigated in detail. By applying a continuous constant heat ramp, a correlation between the appearance of the sharp release of hydrogen in compact material and the film deterioration observed from light microscope images. Moreover, the influence of the film density and morphology on the hydrogen effusion is discussed. In the end, a schematic physical model which can explain the observation is introduced.

2. Experimental Section

Six a-Si:H layers were PECVD deposited on planar silicon monocrystal substrates immediately after the removal of the native oxide in hydrofluoric acid. The used deposition tool was a parallel plate direct plasma reactor with an electrode distance of 22 mm. The gas flux ratios $R_x = [X]/([X] + [SiH_4])$ were $R_{H_2} = 0.5$ and $R_{Ar} = 0.95$ at a pressure of 1 Torr and a plasma power of 10 W for 1500 s, leading to a columnar structure due to the large Ar fraction in the plasma.^[18] The hydrogen concentration was varied using different substrate temperatures T_S during the deposition ranging from 100 to 400 °C and was measured by NRA.^[6] The hydrogen concentrations C_H as well as the film thicknesses d are shown in Table 1. It can be seen when the substrate temperature rises, the hydrogen concentration drops from about 20 to 10 at% and the thickness of the film increases up to a factor of two.

Table 1. The film thicknesses d of PECVD deposited a-Si:H at various substrate temperatures T_S , deposition rate r , and NRA measured hydrogen concentration C_H .^[6]

Sample name	T_S [°C]	d [nm]	r [nm s ⁻¹]	C_H [at%]
A1	100	438	0.29	19.22 ± 0.08
A2	150	526	0.35	17.67 ± 0.08
A3	200	608	0.41	15.61 ± 0.07
A4	250	683	0.46	13.77 ± 0.07
A5	300	724	0.48	12.27 ± 0.06
A6	400	778	0.52	10.09 ± 0.08

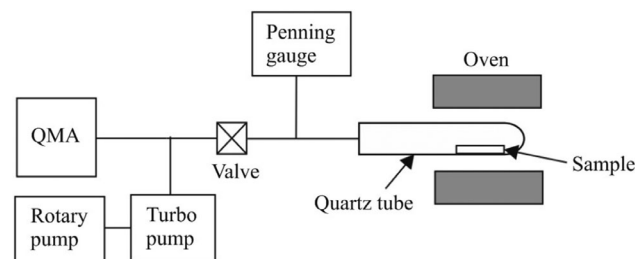


Figure 1. Schematic illustration of the gas effusion mass spectrometer.

3. Hydrogen Effusion Mass Spectroscopy

A schematic illustration of the used gas effusion mass spectrometer is shown in Figure 1. A quadrupole mass analyzer (QMA) was applied to detect the effused gas from the samples with a mass up to 100 amu. Once a sample is loaded in a quartz tube, the system is constantly evacuated using a turbo molecular pump in combination with a rotary pump. To avoid a disturbance of the background signal due to the ambient humidity or desorbed gases from the quartz glass, the apparatus is baked out once the system pumped down to 10⁻⁷ mbar. Following the bake out process, at the pressure of 10⁻⁹ mbar, an empty quartz measurement is carried out and subtracted from the sample measurement data as a background signal.

The a-Si:H-coated silicon wafers were cleaved into 5 mm × 5 mm pieces to be loaded in a quartz tube. For more accurate results, only one sample per run was loaded and the hydrogen effusion of the empty quartz was measured twice. A maximum temperature of 1000 °C was achieved by a constant heating rate of 20 °C min⁻¹. The influence of the annealing treatment T_a on the surface before and after the hydrogen effusion measurements was monitored by optical microscopy. The setup in Figure 1 is a simplified version of the apparatus illustrated in Figure 17.1 in the study by Beyer and Einsele.^[19]

4. Results

4.1. Effusion Measurements

The normalized partial pressure of hydrogen effusion as a function of the annealing temperature T_a is shown in Figure 2 for the a-Si:H films.

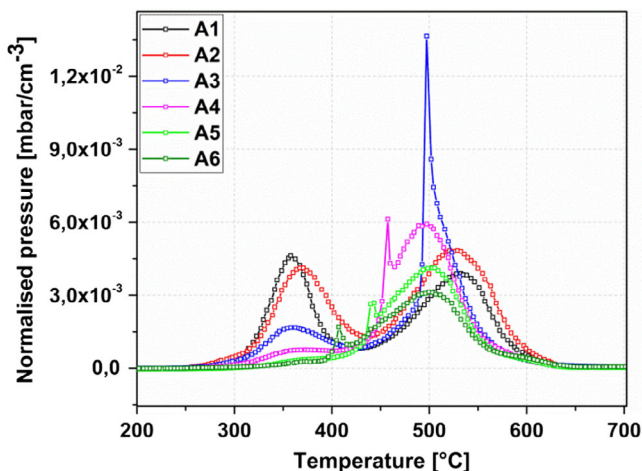


Figure 2. Normalized hydrogen intensity as a function of the annealing temperature T_a resulting from effusion measurement of a-Si:H layers A1–A6. The heat rate was $20\text{ }^\circ\text{C min}^{-1}$.

Table 2. Mean value of the integrated area under the hydrogen effusion spectra, peak position of LT, HT, and SPs of all a-Si:H layers.

Sample name	$A_{H\text{ EFF}}$ [a.u.]	LT [$^\circ\text{C}$]	SP [$^\circ\text{C}$]	HT [$^\circ\text{C}$]
A1	2.21695	357	–	539
A2	2.29774	367	–	528
A3	2.09823	357	497	–
A4	1.81366	373	457	497
A5	1.43484	373	443	505
A6	1.05926	371	407	508

The total effused hydrogen content is equal to the integrated hydrogen partial pressure over the time interval, measured by the quadrupole analyzer.^[19] The peak positions observed in the hydrogen effusion spectra and the mean values for the integrated area under the effusion spectrum $A_{(H, \text{Eff})}$, which is proportional to the hydrogen concentration C_H , are shown in **Table 2**. The values of $A_{(H, \text{Eff})}$ show a reduction of roughly 50% in the hydrogen effusion rate from A1 to A6 (Table 2). These results are proportional to the hydrogen concentrations measured by NRA (Table 1) and will be discussed in other studies. As the substrate temperature T_S is a set temperature of the table heater, it is assumed that the temperature at the substrate surface is lower during deposition and thus it can explain the unexpected lower annealing temperature (LT) peak at T_a of $371\text{ }^\circ\text{C}$ in sample A6.

4.2. The Effusion Spectra in Regard to the Density and Porosity of the a-Si Layer

4.2.1. Introduction of Groups 1 and 2

As shown in Figure 2, the hydrogen effusion spectra can be classified into two groups. Group 1 includes samples A1 and A2, in which the spectrum contains two main effusion peaks, one at LT of about $360\text{ }^\circ\text{C}$ and one at higher temperature (HT) of about $530\text{ }^\circ\text{C}$. However, in group 2, including A3–A6, the HT peaks become the main component of the spectra with a rather small LT peak. The significant change in the spectra in group 2 was the appearance of a SP on the rising edge of the HT peak. To ensure that these SPs were not caused by an artifact introduced by the measurement equipment, the experiments were repeated three times for each sample.

The correlation between the SP in group 2 and the substrate temperature T_S and the anneal temperature T_a in which the peaks occurred during effusion measurement are shown in **Figure 3**. The dash lines are a guide for the eyes. As shown in Figure 3a,

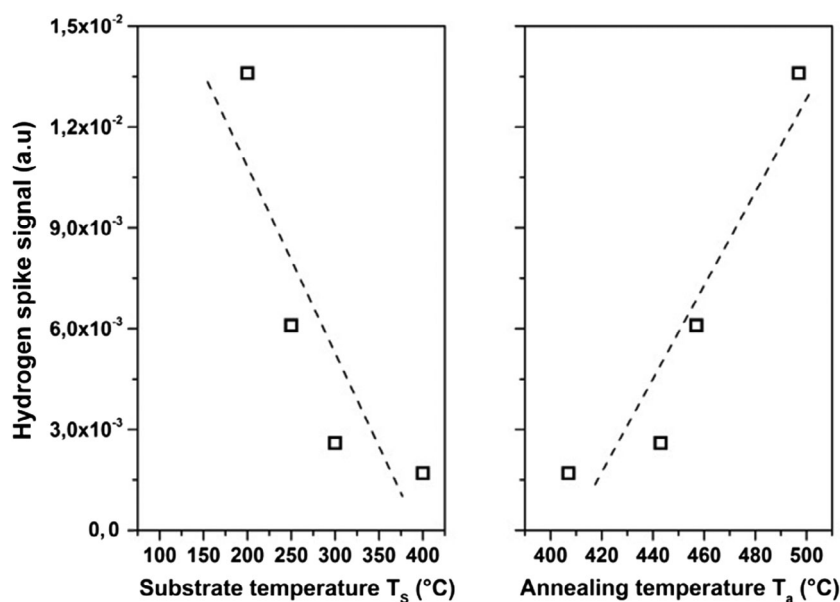


Figure 3. The spike of hydrogen effusion as a function of substrate temperature and annealing temperature.

the SP height decreases with increase in substrate temperature T_S . In contrast, in Figure 3b, the SP signal increases while the peak position shifts to higher annealing temperatures T_a .

4.2.2. Layer Density and Morphology

As shown in Table 1, with deposition at higher substrate temperatures T_S , the hydrogen concentration decreases. In hydrogenated material, the total hydrogen content defines whether the material contains a compact or a void-rich structure. Therefore, there is a link between the variation of effusion curves between the two groups and the change in density and microstructure of the layers.^[19,20] A detailed study of the microstructure of layers deposited at equal deposition conditions was published by Steffens et al.^[21] Therein, FTIR measurements were utilized to determine the hydrogen bond configurations and in turn the microstructure factor R .^[22] This quantity has a value between 0 and 1, where lower values correspond to a more ordered and denser microstructure and larger values to a less ordered and loose structure. A basically decreasing trend was observed with increasing substrate temperature during deposition from $R = 0.5$ in A1 at $T_S = 100^\circ\text{C}$ to $R = 0.3$ in A6 at $T_S = 400^\circ\text{C}$. Thus, the amorphous network can be assumed to be denser for higher T_S .

Without considering the substrate effect which impact the bonding structure at the interface, the hydrogen effusion peaks have been attributed to a surface desorption process within voids followed by rapid out-diffusion of H_2 molecules in the LT process and in the HT range to diffusion of atomic hydrogen by hopping from one bonding site to another.^[7,9,23] Moreover, a model proposed by Smets et al. indicates that the film with high hydrogen concentration and low density contains microscopic voids, while by increasing the film density and lowering the H concentration, vacancies are more likely to dominate.^[14] In addition, the interface bubbles as described by Shanks' model must be considered.^[9] However, the Shanks' samples were prepared by sputter technology and at room temperature.

In "group 1," the low temperature depositions $T_S < 200^\circ\text{C}$ caused a large discontinuity of the Si–Si network due to the high concentration of hydrogen and voids with diameter of few nm.^[21] Such a low-density structure results in spaces wide enough for H_2 molecules to diffuse at low annealing temperatures T_a . It is also known that an effusion peak at T_a of around 350°C can be associated with the hydrogen released from polysilane chain-like sites $(\text{SiH}_2)_n$.^[23,24] During the hydrogen release, the voids collapse and a relatively compact material is formed, so that the diffusion of molecular hydrogen becomes nearly impossible at high T_a . Therefore the second peak at high annealing temperature is almost due to the release of atomic hydrogen.^[12] With regard to the recent view, in a film structure with higher R values and hydrogen concentrations of above 14 at%, the presence of microscopic voids is more likely.^[14,16]

In contrast, in "group 2," by increasing the substrate temperature $T_S > 200^\circ\text{C}$, the growth rate of a-Si film increases, whereas the hydrogen concentration decreases (Table 1). By less diffraction of Si–Si bonds by hydrogen atoms, the microstructure becomes denser and so the number of voids in the microstructure and the size of interface bubbles decreases.^[21] Furthermore, based on the R values resulting from the FTIR analysis, vacancies

in denser layers are dominant than voids. Reduction and disappearance of the LT peak and change of spectrum in a single peak at HT shows the decrease in the number of polysilane chains and hydrogen bonds near the surface. Nevertheless, it suggests that the release of hydrogen mainly occurs in atomic form and from the bonds (Si–H or Si–H₂) almost in the bulk.

4.3. Light Microscope Imaging (Surface Morphology)

To monitor the impact of annealing temperature T_a on surface morphology of a-Si films, surface images were acquired with a light microscope at $50\times$ magnification. The images were obtained from the sample as-deposited and after the effusion measurement, see Figure 4, left and right columns, respectively.

The two groups were separated by the red frames. The microscope images also show that these two groups have different surface morphologies after thermal annealing. The size of interface bubbles as-deposited seems to be in micrometer as shown by others.^[9] It is important to know how the samples react to the high annealing temperature T_a with regard to their different deposition conditions and the corresponding microstructure. In group 1, the surface remained almost unchanged under the exposure of high annealing temperatures T_a during the effusion measurement. However, in group 2, film deterioration was observed after the effusion measurements. It can be seen that the deteriorated film area is increasing from A3 to A6, i.e., with increasing substrate temperature T_S during the film deposition and rise of film density.

With regard to Li et al., blistering and layer delamination were related to the FTIR determined microstructure factor R mentioned earlier.^[25] According to these authors, blistering predominantly occurs for low R values, hence dense amorphous networks are formed. This statement fits well to the increased deteriorated film area with increasing substrate temperature during deposition as the microstructure decreases for similar layers simultaneously.^[21]

Figure 5 shows a cross-sectional image of the sample A1 as-deposited with more details acquired by scanning electron microscopy (SEM), indicating the location of some bubbles at the interface of the a-Si:H/c-Si. The thickness of a-Si was measured in this image of about 477 nm, which is similar to the value in Table 1 measured by Steffens et al.^[6] The dark area indicates the existence of bubbles at the interface. The measured diameter of the bubbles was different and ranged up to 450 nm in this sample. No large bubble in micrometer scale has been found at the interface as shown by the microscopic images in Figure 4 left column.

5. Discussion

The samples A2 and A4, respectively, were picked as representatives from groups 1 and 2 for a detailed study of their different thermal behaviors.

5.1. Hydrogen Effusion in Group 1

Figure 6a shows the peak deconvolution with Gaussian curve fitting for the spectrum of sample A2. Gaussian fitting of the

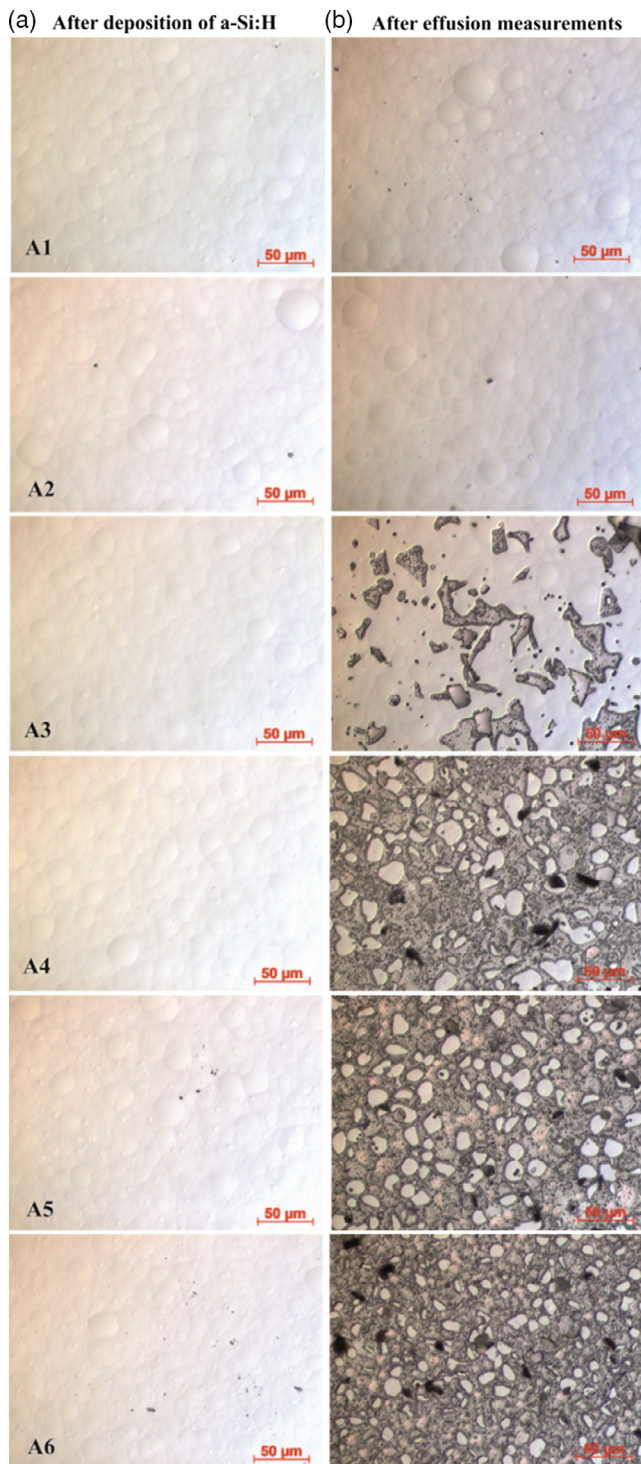


Figure 4. Light microscope images of sample's surfaces acquired before (left column) and after (right column) effusion measurements.

curves was used to simplify the interpretation of differences in the effusion spectra. A list of the peak positions and the percentage fraction of integrated area among the peaks is shown in **Table 3**. As the temperature is measure of kinetic

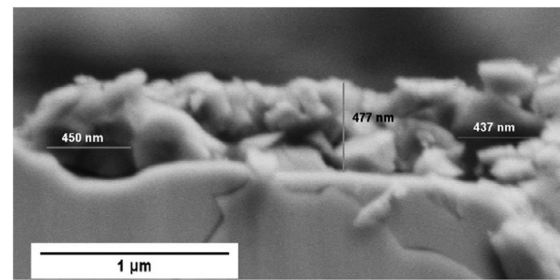


Figure 5. A cross-sectional view of the sample A1 as-deposited obtained by SEM.

energy, the peaks revealed under the spectrum indicate the release of hydrogen from various hydrogen bond sites due to the different bond rupture energies.^[24] However, in a system with a diffusion-limited effusion, it is almost impossible to evaluate the origin of the peaks in detail. This means, for example, that the Si–H binding energy does not directly determine the effusion temperature, but rather the energy of the entire diffusion process including bond ruptures and bond reconstructions. Another effect is the densification due to annealing during effusion measurement which occurs in all samples which shift the HT effusion peak to higher annealing temperatures T_a as the hydrogen diffusion process changes from molecular to atomic form.^[12] The role of densification can be larger in a low density film such as A2. Moreover, the model proposed by Macco et al. suggests a time-dependent immigration of nanoscale vacancies due to annealing at LTs (300 °C) associated with the hydrogen diffusion through the film.^[26] However, this work was performed under different deposition conditions.

The effusion spectrum of A2 (Group 1) shows a smooth release of hydrogen with two main peaks. As discussed earlier, a large number of voids are expected in this group. In addition, a high concentration of hydrogen in this film increases the possibility of H_2 release from polysilane structure at low annealing temperatures T_a .^[23] Therefore, the initial release of hydrogen in A2 is at T_a of 294 °C and follows by a large LT peak at 367 °C which contains the 50% of total amount of hydrogen in the film (Table 3).

The formation of bubbles at the interface is known to be substrate dependent. For example, it is reported that substrates such as c-Si and sapphire usually lead to bubble formation, while quartz glass does not cause such bubbles.^[9,23] Shanks and Ley proposed a proportional relation between number of the interface bubbles and the hydrogen concentration in the a-Si:H.^[9] It means that A2 with high concentration of H ($\approx 18\%$) must contain large number of bubbles which facilitate diffusion procedure. Moreover, low substrate temperature T_S results in a larger size of bubbles at the interface of a-Si/c-Si.^[21] Of most importance is that the presence of numerous bubbles and voids are likely the diffusion paths in A2 and can be a reason why no film deterioration occurs.

Other than that, the impact of film thickness on the size of interface bubbles must be considered. As Shanks and Ley reported, the rise of film thickness increases the bubble diameter.^[9] However, we cannot confirm the increase in bubble's diameter from A1 to A6 in Figure 4 but the assumption is that by increase

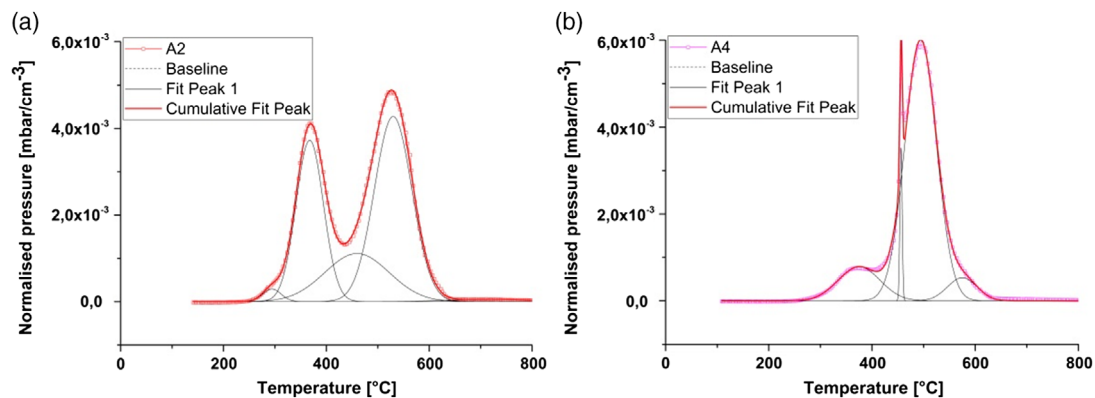


Figure 6. Gaussian fit of the hydrogen evolution spectra of a) sample A2 from group 1 and b) sample A4 from group 2.

Table 3. Peak position and normalized integrated effusion intensity for the Gaussian components of effusion spectra of samples A2 and A4.

Sample name	Peak I [°C]	Norm. area [%]	Peak II [°C]	Norm. area [%]	Peak III [°C]	Norm. area [%]	Peak IV [°C]	Norm. area [%]	Peak V [°C]	Norm. area [%]
A2	294	2.6	367	29.8	459	20.8	529	46.8	–	–
A4	–	–	375	13	456	3.8	500	76.9	579	6.3

in substrate temperature T_S improves the sticking of a-Si:H to c-Si surface and so the diameter of the interface bubbles decreases, whereas the thickness increases.^[20,27]

5.2. The Cause of the SPs in Group 2

Figure 6b likewise presents the fitting curve of sample A4 from Group 2. The effusion curve shows the LT peak at 375 °C which drops to less than 20% of total amount of hydrogen in film. As a major change in this sample, a SP is observed at 456 °C, followed by a large HT peak. It shows that 80% of the total hydrogen in A4 is released during and after the occurrence of a SP at high annealing temperatures T_a of more than 400 °C. After desorption of near-surface molecular hydrogen during LT, the atomic release of hydrogen at HT is limited by diffusion through a thicker layer. Considering of A4 as a denser and thicker a-Si:H film due to the higher substrate temperature T_S and dominance of vacancies instead of voids implies that the structure inhibits the release of hydrogen.^[14,15] The hydrogen atoms must hop from one bond to another and diffuse either through the layer to the interface of a-Si/c-Si or the surface of a-Si and effuse out the sample. The atomic hydrogens, which collect on the surface of the interface bubbles as a dominant cavity in a compact structure, are desorbed into the bubble in the form of molecular H_2 , see Figure 7a. The excessive pressure of stored hydrogens leads to a local explosion and film delamination. The increase in pressure to the critical point P_{cr} and the deterioration of the film due to the abrupt hydrogen release are shown in Figure 7b,c, respectively. These figures illustrate schematically the layer structure where sizes and appearance are neglected. It must be considered that the effusion measurement was carried out in vacuum and so that P_{cr} is relatively low. Once the bubbles have exploded, the rest of

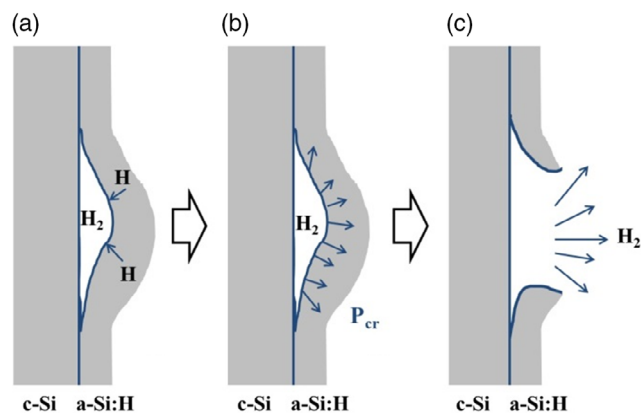


Figure 7. The visual model of sharp release of hydrogen due to the excessive pressure inside small bubble in a film deposited at high substrate temperature $T_S > 200$ °C which causes the film damage.

the hydrogen diffuses as usual in form of a smooth HT release which begins immediately after the SP.

The other possibility is that the size of deteriorated film due to the explosion depends on the size of the interface bubbles and the hydrogen concentration.

If the volume of bubbles decreases due to the high density, whereas film contains low H concentration, the number of hydrogens stored in the bubble would be less and therefore the hydrogen release during explosion (delamination) decreases, hence the corresponding area under the SP reduces.^[21] It can explain why the SP becomes smaller from A3 to A6 as the hydrogen concentration decreases and films get denser. The shift in the position of the SP can be attributed to the diameter of interface voids. We believe that the temperature difference between

the LT peak position and the SP shows the time required to fill the voids before the explosion occurs, which decreases from A3 to A6. It proposes that the volume of bubble reduced from A3 to A6 which disagrees with the proportional relation between the bubble diameter and the film thickness claimed by Shanks and Ley.^[9] A reason for the different result might be the various layer preparations, where Shanks and Ley's samples were sputtered at room temperature, and the presented samples were deposited by PECVD at elevated temperatures of 100–400 °C.^[9]

Based on the schematic models and the curve simulations, it can be concluded that the hydrogen effusion is divided into four steps: 1) Thermal-driven breakage of hydrogen bonds from the original binding with chemical potential of μ_{H} . 2) Diffusion of hydrogen with diffusion energy of E_{D} . 3) Chemical reaction between the atomic hydrogen and formation of H_2 . 4) (a) In a low-density film, H_2 molecules diffuse through the porosity to the surface and effusing out without causing a surface damage in the form of smooth LT and HT peaks. (b) In a compact film after desorption of near surface hydrogen as LT peak, the potential energy of stored hydrogen molecules N_{H} in bubbles located at interface with volume of V_{bubble} converts to a kinetic energy of the effused hydrogen at SP temperature T_{SP} (explosion) and heat Q .

Time to fill the bubble is indicated by the difference between LT and SP peak position, which is associated with the size of the bubble.

6. Conclusion

a-Si:H films were deposited on c-Si surfaces at different substrate temperatures T_{S} by PECVD technology, and the role of micro-structure and hydrogen concentration on the hydrogen effusion spectra during annealing was investigated. Two groups were identified after the effusion measurements. The low-density porous structure of group 1 ($T_{\text{S}} < 200$ °C) resulted in a smooth effusion curve with two main peaks. While in group 2 ($T_{\text{S}} \geq 200$ °C) by the increase in film density, hydrogen effusion at LT decreases and a SP has been observed during the effusion measurement. Along with the SP, film deterioration was revealed after effusion measurement. An explanation for the appearance of sharp effusion peaks in compact material (group 2) is that the diffusion of free hydrogen near substrate to the interface bubbles is favorable which form the H_2 molecules introducing a high pressure in these bubbles. The excessive pressure in a small volume of the voids leads to local explosion (film delamination) and abrupt release of hydrogen. Moreover, the distance between the LT and SP peak position decreases by the increase in substrate temperature T_{S} . It is evident that the increase in the film density decreases the size of interface bubbles. The area under the SP decreases as the hydrogen concentration reduces in the film and the bonding structure to the substrate improves.

Acknowledgements

The authors gratefully thank Dr. Wolfhard Beyer from Jülich research center for his valuable discussion and feedbacks on this research. This work was carried out within the joint research graduate school "StrukturSolar II" of Anhalt University of Applied Sciences and Martin-Luther-University

Halle-Wittenberg which is funded by the German Ministry of Education and Research under identification code 03EK3570A.

Conflict of Interest

The authors declare no conflict of interest.

Keywords

a-Si:H films, hydrogen effusion, interface voids

Received: February 20, 2020

Revised: April 28, 2020

Published online: May 28, 2020

- [1] A. G. Aberle, *Sol. Energy Mater. Sol. Cells* **2001**, 65, 239.
- [2] W. A. Lanford, M. J. Rand, *J. Appl. Phys.* **1978**, 49, 2473.
- [3] S. A. Schwarz, *Encyclopedia of Materials: Science and Technology*, 2nd ed., Science Direct, Bellcore, Red Bank, NJ **2001**, pp. 8283–8290.
- [4] A. E. T. Kuiper, *Surf. Interface Anal.* **1990**, 16, 29.
- [5] S. Gerke, H. W. Becker, D. Rogalla, R. Job, B. Terheiden, *Phys. Status Solidi RRL* **2016**, 10, 828.
- [6] J. Steffens, H. W. Becker, S. Gerke, S. Joos, G. Hahn, B. Terheiden, *Energy Procedia* **2017**, 124, 180.
- [7] W. Beyer, *Phys. Status Solidi A* **2016**, 213, 1661.
- [8] S. Jafari, J. Hirsch, D. Lausch, M. John, N. Bernhard, S. Meyer, *AIP Conf. Proc.* **2019**, 2147, 050004.
- [9] H. R. Shanks, L. Ley, *J. Appl. Phys.* **1981**, 52, 811.
- [10] S. Lebib, P. R. i Cabarrocas, *Eur. Phys. J. Appl. Phys.* **2004**, 26, 17.
- [11] C. Roch, J. C. Delgado, *Thin Solid Films* **1992**, 221, 17.
- [12] W. Beyer, *Thin Solid Films* **1982**, 90, 145.
- [13] A. H. Mahan, W. Beyer, D. L. Williamson, J. Yang, S. Guha, *Philos. Mag. Lett.* **2000**, 80, 647.
- [14] A. H. M. Smets, W. M. M. Kessels, M. C. M. Van de Sanden, *Appl. Phys. Lett.* **2003**, 82, 1547.
- [15] A. H. M. Smets, M. C. M. Van De Sanden, *Phys. Rev. B* **2007**, 76, 073202.
- [16] J. Melskens, A. H. M. Smets, M. Schouten, S. W. H. Eijt, H. Schut, M. Zeman, in *IEEE 38th Photovoltaic Specialists Conf. (PVSC) Part 2*, IEEE, Piscataway, NJ **2012**, pp. 1–8.
- [17] J. Melskens, S. W. H. Eijt, M. Schouten, A. S. Vullers, A. Mannheim, H. Schut, B. Macco, M. Zeman, A. H. M. Smets, *IEEE J. Photovoltaics* **2017**, 7, 421.
- [18] S. Gerke, H. W. Becker, D. Rogalla, G. Hahn, R. Job, B. Terheiden, *Energy Procedia* **2015**, 77, 791.
- [19] W. Beyer, F. Einsele, *Advanced Characterization Techniques for Thin-Film Solar Cells* (Eds: D. Abou-Ras, T. Kirchartz, U. Rau), Wiley-VCH, Weinheim, Germany **2016**, Vol. 2, p. 569.
- [20] W. Beyer, H. Wagner, *J. Non-Cryst. Solids* **1983**, 59, 161.
- [21] J. Steffens, J. Rinder, G. Hahn, B. Terheiden, *J. Non-Cryst. Solids X* **2020**, 5, 100044.
- [22] J. Mouro, A. Gualdino, V. Chu, J. P. Conde, *J. Appl. Phys.* **2013**, 114, 184905.
- [23] W. Beyer, H. Wagner, *J. Phys. Colloq.* **1981**, 42, 783.
- [24] D. K. Biegelsen, R. A. Street, C. C. Tsai, J. C. Knights, *Phys. Rev. B* **1979**, 20, 4839.
- [25] S. Li, M. Pomaska, J. Hoß, J. Lossen, F. Pennartz, M. Nuys, R. Hon, A. Schmalen, J. Wolff, F. Finger, U. Rau, *Appl. Phys. Lett.* **2019**, 114, 153901.
- [26] B. Macco, J. Melskens, N. J. Podraza, K. Arts, C. Pugh, O. Thomas, W. M. M. Kessels, *J. Appl. Phys.* **2017**, 122, 035302.
- [27] A. Matsuda, K. Nomoto, Y. Takeuchi, A. Suzuki, A. Yuuki, J. Perrin, *Surf. Sci.* **1990**, 227, 50.